

TABLE 1
Nutrient and Energy Composition of Custom Diets

	Isocaloric, fat-adjusted diets			Constant fat, carbohydrate-adjusted diets			
	Chow	% Fat			% Carbohydrate		
		5%	10%	15%	50%	60%	70%
Metabolizable energy (kcal/g)	3.1	3.7	3.7	3.7	3.3	3.7	4.1
% by weight							
Fat	6.4	5	10	15	6.6	6.6	6.6
Protein	24.3	18.3	18.3	18.3	18.3	18.3	18.3
Carbohydrate	38.7	63.6	52.4	41.1	48.6	59	68.6
Fiber	11.3	3	10.5	18	18	7	—

MATERIALS AND METHODS

Animal handling. C57BL/6 ovariectomized (ovx) female mice were obtained from Charles Rivers Laboratories (Portage, MI) on postnatal day (PND) 25 with body weights within 10% of the mean body weight upon arrival. B6.129-*Scd1^{tm1Mz}/J* heterozygous mice (Miyazaki *et al.*, 2001) (Jackson Laboratory, Bar Harbor, ME) had free access to chow or custom diets and water upon arrival and throughout the study. On PND 21, mice were genotyped and weaned. Mice were maintained on a 12-h light/dark cycle and housed in standard cages containing Aspen woodchips. B6.129-*Scd1^{tm1Mz}/J* heterozygous mice were fed Harlan Teklad 7964 F6 Rodent diet (chow). All procedures were carried out with All-University Committee on Animal Use and Care approval.

Diet compositions. Custom diets consisted (by weight) of 19.6% protein, 5, 10, and 15% fat with decreasing carbohydrate (68, 56, and 44%) for an isocaloric intake of 3.7 kcal/g (Table 1). Carbohydrate-adjusted diets consisted (by weight) of constant fat and protein (6.6 and 19.6%, respectively) with increasing total carbohydrate content of 50, 60, and 70% for total caloric intakes of 3.3, 3.7, and 4.1 kcal/g, respectively (Table 1). Custom diets use different ingredients compared with standard chow, which confounds comparisons to other studies. Specifically, custom diet formulations use purified ingredients. In contrast, chow (31% protein, 19% fat, and 50% carbohydrate calories by weight) consists of a proprietary blend of soybean meal, ground corn, wheat, fishmeal, soybean oil, whey, brewer's yeast, and other vitamins and minerals.

Diet study in vivo treatment. On PND 28, mice fed with custom diets ($n = 5$) were gavaged with 0.1 ml of sesame oil (vehicle control) or 30 μ g TCDD (Dow Chemical Company, Midland, MI) per kg body weight. Immature ovx mice were used to facilitate comparisons with other data sets, as well as to minimize potential interactions with estrogens from maturing ovaries. The dose was chosen to elicit moderate hepatic effects while avoiding overt toxicity. Animals were sacrificed at 24 and 168 h postdose, weighed, and blood was collected via submandibular vein puncture before sacrifice. Tissue samples were removed, weighed, flash frozen in liquid nitrogen, and stored at -80°C .

Gas chromatography mass spectrometry fatty acid methyl ester hepatic lipid profiling. Hepatic lipid analysis was performed as previously described (Angrish *et al.*, 2011) and as described in Supplementary data. Briefly, liver lipids were extracted by Folch method, dried down under nitrogen, converted to methyl esters and resuspended in hexane. Samples were separated and analyzed by gas chromatography mass spectrometry (GC-MS). 19:1n9 free FA (FFA) and 19:0 TAG were added as extraction efficiency controls, and 17:1n1 FAME (Nu-chek, Elysian, MN) was spiked in as a loading control. Data were analyzed with QuanLynx software and reported as $\mu\text{mol/g}$ liver tissue. FA levels are based on peak areas from total ion chromatograms and $\mu\text{mol/g}$ is obtained from a linear calculation of a calibration curve normalized to sample weight.

¹⁴C-Oleate studies. On PND 28, *Scd1* wild type and null mice ($n = 5$) were gavaged with sesame oil or 30 $\mu\text{g/kg}$ TCDD. 4 h before sacrifice at 120 h, mice

were gavaged with 2 μCi ¹⁴C-oleate (0.1 ml of 20 $\mu\text{Ci/ml}$ in sesame oil; ARC 0297; American Radiolabeled Chemicals, St Louis, MO). Blood was collected from the saphenous vein at 0.5, 1, and 2 h after ¹⁴C-oleate gavage or the submandibular vein at 4 h. Tissues were harvested, weighed, flash frozen in liquid nitrogen, and stored at -80°C . Duodenum (~3.5 cm) and jejunum (~6 cm) sections were collected, flushed with phosphate buffered saline, and cut longitudinally. Intestinal epithelium were scraped into vials containing ~1.0 ml of TRIzol (Invitrogen, Carlsbad, CA), snap-frozen in liquid nitrogen, and stored at -80°C . For fecal pellet analysis, mice were gavaged with 2 μCi ¹⁴C-oleate 120 h post-TCDD dose, and all fecal matter was collected until 48 h after ¹⁴C-oleate gavage.

Liver, parametrial adipose, and muscle samples were homogenized in Folch solution (2:1 chloroform:methanol), 0.2 ml 40% methanol was added, vortexed, and centrifuged at $10,000 \times g$ for 5 min. The organic phase was dried under nitrogen and resuspended in hexane. Samples were directly added to 10 ml liquid scintillation fluid (Safety-Solve, RPI, Mount Prospect, IL), and ¹⁴C levels counted on a Packard Tri Carb Liquid Scintillation Counter (PerkinElmer; Waltham, MA). Each sample was spiked with 17:1n1 FAME (Nu-chek; Elysian, MN) to control for extraction efficiency and quantified by GC-MS. Liver and adipose samples were normalized to sample weight \times whole organ weight. Muscle samples were normalized to sample weight. For ¹⁴C levels in fecal pellets, ~30 μg dried pellets were ground to a fine powder with mortar and pestle and added to 10 ml liquid scintillation fluid. Fecal samples were normalized to total dry fecal pellet weight. For ¹⁴C levels in serum, 5 μl of serum was added directly to scintillation cocktail. Samples were normalized to the average body weight of each mouse.

Quantitative real-time PCR. RNA was isolated from frozen liver samples and intestinal scrapings, and quantitative real-time PCR (QRT-PCR) expression was performed as previously described (Boverhof *et al.*, 2006). The copy number of each sample was standardized to the geometric mean of glyceraldehyde-3-phosphate dehydrogenase (*Gapdh*), hypoxanthine guanine phosphoribosyl transferase (*Hprt*), and beta actin (*Actb*) to control for differences in RNA loading, quality, and cDNA synthesis (Vandesompele *et al.*, 2002). Data are reported as the fold change of standardized treated over standardized vehicle values (Supplementary table 5 provides a complete list of gene names and abbreviations).

Statistical analysis. Data were analyzed by analysis of variance (ANOVA) followed by Tukey's *post hoc* test in SAS V9.2 (SAS Institute, Cary, NC). Differences between treatment groups were considered significant when $p < 0.05$.

RESULTS

Body and Liver Weights

Mice fed with fat-adjusted diets had increased relative liver weights (RLWs) (see Supplementary table 1) at 24 and 168 h

TABLE 2
Hepatic Lipid Levels in Mice Fed With Fat- or Carbohydrate-Adjusted Diets 168 h Post 30 μ g/kg TCDD Dose

		% Fat		
		5%	10%	15%
A. Fat-adjusted diet				
A. Fat-adjusted diet	Treatment	5%	10%	15%
Total FA	Vehicle	135.6 \pm 16.7	113.5 \pm 9.5	96.3 \pm 7.1****
	TCDD	195.0 \pm 14.0*	194.3 \pm 16.4*	188.0 \pm 15.6*
Total SFA	Vehicle	40.9 \pm 3.3	41.9 \pm 3.8	36.6 \pm 2.0
	TCDD	53.9 \pm 3.3***	53.8 \pm 1.4*	47.7 \pm 3.8*
Total MUFA	Vehicle	54.1 \pm 12.1	31.0 \pm 4.8****	18.2 \pm 2.8****
	TCDD	92.6 \pm 12.0***	66.0 \pm 11.0*	54.8 \pm 7.3*
Total PUFA	Vehicle	33.2 \pm 2.7	40.6 \pm 2.6	41.5 \pm 2.9
	TCDD	47.7 \pm 2.8****	74.4 \pm 4.4***	85.5 \pm 7.2*
B. Carbohydrate-adjusted diet				
		% Carbohydrate		
		50%	60%	70%
Total FA	Vehicle	108.8 \pm 24.6	113.0 \pm 4.7	135.9 \pm 9.8
	TCDD	156.8 \pm 7.6*	148.6 \pm 22.3**	193.0 \pm 34.8*
Total SFA	Vehicle	45.1 \pm 7.74	46.7 \pm 3.2	49.7 \pm 4.9
	TCDD	54.3 \pm 2.7	51.0 \pm 5.4**	64.5 \pm 8.7*
Total MUFA	Vehicle	28.4 \pm 11.6	31.0 \pm 2.6	51.2 \pm 6.1
	TCDD	50.7 \pm 5.5**	51.3 \pm 12.8	79.8 \pm 26.0*
Total PUFA	Vehicle	35.4 \pm 5.6	35.3 \pm 3.3	35.0 \pm 2.4
	TCDD	51.8 \pm 2.5*	46.3 \pm 4.9*	48.7 \pm 5.0*

Note. A. Fat-adjusted diet: * p < 0.05 for TCDD compared with vehicle within a diet, ** p < 0.05 for TCDD 15% fat compared with TCDD 5 or 10%, *** p < 0.05 for TCDD 5% fat compared with TCDD 10%, **** p < 0.05 for vehicle 5% compared with vehicle 10% or 15%, n = 5.

B. Carbohydrate-adjusted diet: * p < 0.05 for TCDD compared with vehicle within a diet, ** p < 0.05 for TCDD 70% carbohydrate compared with TCDD 50 or 60% carbohydrate, n = 5.

following a single oral gavage of 30 μ g/kg TCDD. In contrast, mice fed with carbohydrate-adjusted diets exhibited increased RLW at 168 h only. There were no significant alterations in body weight or body weight gain throughout the study, suggesting treatment had no effect on feed consumption.

Hepatic Lipid Content in Mice Fed With an Isocaloric, Fat-Adjusted Diet

Vehicle-treated mice exhibited a dose-dependent decrease in TFAs primarily due to decreases in MUFAs (Table 2A). However, TCDD increased TFAs 1.4-, 1.7-, and 2.0-fold in mice fed with 5, 10, and 15% fat diets, respectively (Fig. 1A), compared with diet-matched vehicles. More specifically, absolute levels of saturated FA (SFA), MUFA, and polyunsaturated FA (PUFA) increased with palmitic (16:0) and oleic (18:1n9) acids representing 80–90% of all hepatic SFAs and MUFAs, respectively (Supplementary table 2). Note that palmitic and oleic acids represent > 66 and > 98% of dietary SFAs and MUFAs, respectively, in the fat-adjusted diets (Supplementary table 3A), with absorption efficiencies of > 90% (Labonte *et al.*, 2008).

Hepatic PUFAs also exhibited a dose-dependent increase in dietary fat (Table 2A) primarily due to linoleic acid (18:2n6) accumulation (Fig. 1B). 18:2n6, which represents ~65% of all hepatic PUFAs, is an essential FA that can only be acquired from the diet with a reported absorption efficiency of > 95% (Labonte *et al.*, 2008). α -Linolenic acid (18:3n3), another dietary essential FA, exhibited similar hepatic increases with increasing dietary

fat content that was further induced by TCDD (Fig. 1C). 18:2n6 and 18:3n3 represent > 99% of the PUFA content in isocaloric, fat-adjusted diets (Supplementary table 3A). These results suggest that AhR activation enhances dietary fat processing and/or transport that contributes to TCDD-elicited hepatic steatosis.

Hepatic Lipid Content in Mice Fed With a Constant Fat, Carbohydrate-Adjusted Diet

Mice fed with 50, 60, or 70% carbohydrate diets did not exhibit a dose-dependent increase in hepatic TFA following TCDD treatment. TCDD induced TFAs ~1.4-fold across all carbohydrate-adjusted diets (Fig. 1D). Absolute SFA and MUFA levels increased 1.3- and 1.6-fold, respectively, in mice fed with 70% carbohydrate diet compared with controls (Table 2B). 16:0, 18:1n9, and 18:2n6 were the predominant hepatic SFA, MUFA, and PUFA species, respectively, similar to the composition in mice fed with fat-adjusted diets (Supplementary table 4). However, 18:2n6 and 18:3n3 levels, the essential dietary FAs, remained constant across TCDD-treated mice on carbohydrate diets (Figs. 1E and 1F), suggesting dietary carbohydrate is not a significant contributor to AhR-mediated steatosis.

¹⁴C-Oleate Studies

Lipid accumulation in the liver was investigated in Scd1 wild type and null mice gavaged with 2 μ Ci ¹⁴C-oleate 5 days

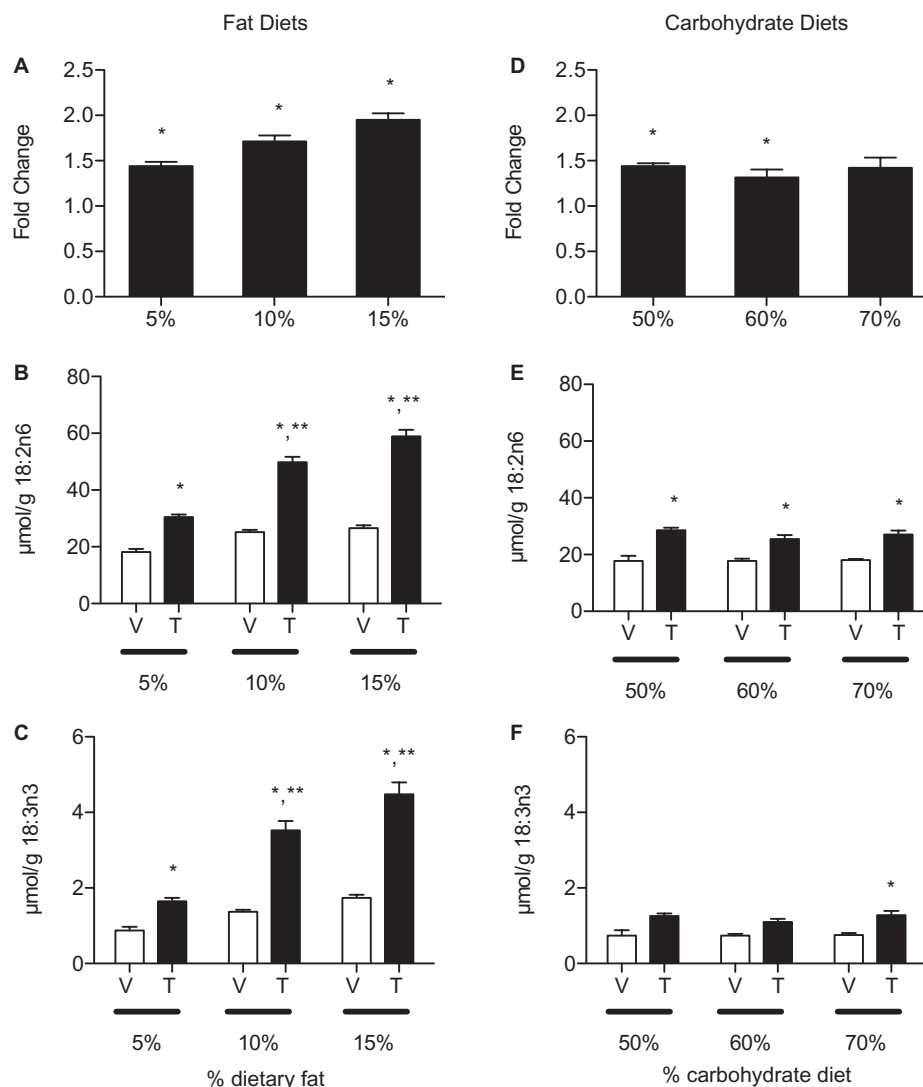


FIG. 1. Hepatic absolute and essential FA levels in mice fed with increasing fat or carbohydrate diets treated with sesame oil vehicle (V) or 30 $\mu\text{g}/\text{kg}$ TCDD (T) for 168 h. (A–C) Mice fed with 5, 10, and 15% fat diet, (A) total fatty acids (TFA), (B) α -linoleic acid (18:2n6), and (C) α -linolenic acid (18:3n3) levels. * $p < 0.05$ for TCDD compared with vehicle within a diet; ** $p < 0.05$ for TCDD 15% fat or 10% fat compared with TCDD 5% fat. (D–F) Mice fed with 50, 60, and 70% carbohydrate diet, (D) TFAs, (E) 18:2n6, and (F) 18:3n3. * $p < 0.05$ for TCDD compared with vehicle within a diet; ** $p < 0.05$ for TCDD 70% carbohydrate compared with TCDD 50% carbohydrate. (A–F) Bars represent mean \pm standard error of the mean (SEM), $n = 5$.

postdose with 30 $\mu\text{g}/\text{kg}$ TCDD. *Scd1* performs the rate-limiting step in MUFA synthesis. Therefore, null mice are incapable of desaturating 18:0 to 18:1n9, yet 18:1n9 is still available via the diet (Supplementary table 3). ^{14}C -levels in hepatic lipid extracts increased twofold and 2.4-fold in TCDD-treated wild type and *Scd1* null mice, respectively (Fig. 2A). This increase is consistent with the approximately twofold oleate increase in mice fed with fat- or carbohydrate-adjusted diets (Supplementary tables 2 and 4), and the approximately threefold increase in 18:1n9 levels in TCDD-treated *Scd1* wild type and null mice (Fig. 2B) (Angrish *et al.*, 2011). The absorption efficiency of oleate is reported to be $> 95\%$ (Labonte *et al.*, 2008). Furthermore, oleate represents $> 90\%$ of

total MUFAs in treated mouse livers (Fig. 2C) (Angrish *et al.*, 2011). TCDD increased serum (1.4-fold) and muscle (1.2-fold) and decreased adipose (-1.3 -fold) and stool (-1.5 -fold) ^{14}C levels, although statistical significance was not achieved (Supplementary figs. 1A–D).

Differential Intestinal and Hepatic Gene Expression

To further examine the effect of AhR activation on dietary lipid uptake, intestinal and hepatic gene expression was examined. Of the genes examined, $> 80\%$ contained a putative, functional DRE (matrix similarity score > 0.847) and/or had hepatic AhR enrichment in ChIP-chip analysis (Table 3) (Dere *et al.*, 2011a,b).

TABLE 3
DREs^a and Regions of AhR Enrichment^b in TCDD Responsive Genes Associated With Lipid and Carbohydrate Transport and Metabolism

Gene ID	Gene symbol	Liver	Duodenum	Jejunum	** of DREs ^a	ChIP peaks 2 h ^b	Function ^c	Regulated by ^c
<i>Xenobiotic metabolism</i>								
13076	<i>Cyp1a1</i>	5799*	222*	22.7*	7	4	Xenobiotic metabolism	AhR
<i>Fatty acid and triglyceride synthesis</i>								
14104	<i>Fasn</i>	-2.8*	NC	NC	4	1	Fatty acid synthesis	SREBP, TR, LXR, cAMP, AMPK
153674	<i>Acly</i>	-2.6***	nd	nd	0	0	Citrate metabolism	Oxaloacetate, ATP
107476	<i>Acaca</i>	-1.4***	nd	nd	3	5	Malonyl CoA acylation	glucagon
68393	<i>Mogat1</i>	3.6*	NC	NC	1	0	Triglyceride synthesis	PPAR, CEBP
233549	<i>Mogat2</i>	3.0*	NC	1.4*	4	3		
13350	<i>Dgat1</i>	2.0	1.4	1.6*	4	0		
67800	<i>Dgat2</i>	1.3	1.4	1.6	2	7		
<i>Fatty acid transport</i>								
238055	<i>Apob</i>	2.5*	NC	1.8*	2	0	VLDL and chylomicron assembly	APOBEC-1
16835	<i>Ldlr</i>	3.2*	2.3*	NC	2	4	Lipoprotein uptake	LXR
12491	<i>Cd36</i>	4.4*	2.7*	NC	0	1	Fatty acid uptake	PPAR, CEBP α , AMPK
26457	<i>Slc27a1</i>	-2.9*	2.3*	-5.8**	2	0	Mitochondrial β -oxidation	PPAR α , PPAR γ
26568	<i>Slc27a3</i>	2.7*	NC	NC	1	0	Unknown	
26569	<i>Slc27a4</i>	3.0*	1.4**	1.4**	0	0	Peroxisomal β -oxidation, CHOL-ester synthesis	PPAR γ , SREBP1c
14080	<i>Fabp1</i>	2.9*	1.4*	1.7*	2	4	TAG synthesis, β -oxidation	PPAR α , HNF4 α
11770	<i>Fabp4</i>	1.4**	1.5	2.5	0	0	Chylomicron assembly	cJun, PPAR γ
117147	<i>Acsm1</i>	-2.0***	nd	nd	3	0	Medium-chain fatty acid transport (mitochondrial β -oxidation)	Acetyl-CoA, malonyl-CoA, NADPH, NADH
233799	<i>Acsm2</i>	-1.5***	nd	nd	0	0		
20216	<i>Acsm3</i>	-1.6***	nd	nd	2	0		
233801	<i>Acsm4</i>	-1.2***	nd	nd	0	0		
14081	<i>Acs11</i>	-1.4***	nd	nd	6	5	Long-chain fatty acid transport (mitochondrial β -oxidation)	
74205	<i>Acs13</i>	-2.3***	nd	nd	0	0		
50790	<i>Acs14</i>	-1.3***	nd	nd	0	2		
<i>Fatty acid metabolism</i>								
16956	<i>Lpl</i>	3.2***	nd	nd	2	0	TAG metabolism of lipoproteins and chylomicrons	Insulin, glucagon, epinephrine
109791	<i>Clps</i>	2.6***	nd	nd	0	0		
18946	<i>Pnliprp1</i>	3.7***	nd	nd	0	0		
11343	<i>Mgll</i>	1.4***	nd	nd	9	0	Monoglyceride metabolism	PPAR α
116939	<i>Pnpla3</i>	-3.3***	nd	nd	0	1	TAG metabolism	
<i>Glycolysis/Gluconeogenesis/Glycogen synthesis</i>								
18534	<i>Pck1</i>	-2.0***	nd	nd	0	1	Gluconeogenesis	Insulin, glucagon, cAMP
14377	<i>G6pc</i>	-2.7***	nd	nd	1	5		Insulin, glucose
18563	<i>Pcx</i>	-1.3***	nd	nd	5	4		ATP
103988	<i>Gck</i>	-1.5***	nd	nd	3	2	Glucose metabolism	G6P, insulin, glucagon
212032	<i>Hk3</i>	2.2***	nd	nd	1	0		
232493	<i>Gys2</i>	-1.5***	nd	nd	2	4		

Note. NC, no change; nd, not detected.

^aDRE distributions were previously determined (Dere *et al.*, 2011a). Only DREs satisfying a matrix similarity score of ≥ 0.85 were included.

^bAhR enrichment was previously determined (Dere *et al.*, 2011b).

^cData from Boron and Boulpaep (2008), Hardwick *et al.* (2009), and Watkins (2008).

* $p < 0.05$ or ** $p < 0.01$ for TCDD compared with vehicle, QRTPCR data at 24 h postdose. QRTPCR data were analyzed by Dunnett's t -test, $n = -5$. *** for $P_1(t) \geq 0.999$ for microarray data at 168 h postdose (Dere *et al.*, 2011a).

Dietary FAs (> 16C) hydrolyzed from TAG by gastric and pancreatic lipases in the intestinal lumen are actively transported into enterocytes before export into the lymphatic and systemic circulation (Iqbal and Hussain, 2009). In the duodenum, TCDD induced low-density lipoprotein receptor (*Ldlr*, 2.3-

fold), Cd36 antigen (*Cd36*, 2.7-fold), and solute carrier family 27 (FA transporter), member 4 (*Slc27a4*, 1.4-fold), as well as FA binding protein 1, liver (*Fabp1*, 1.4-fold), and FA binding protein 4, adipocyte (*Fabp4*, 1.4-fold) (Table 3). Although implicated in mitochondrial β -oxidation (Hardwick *et al.*, 2009;

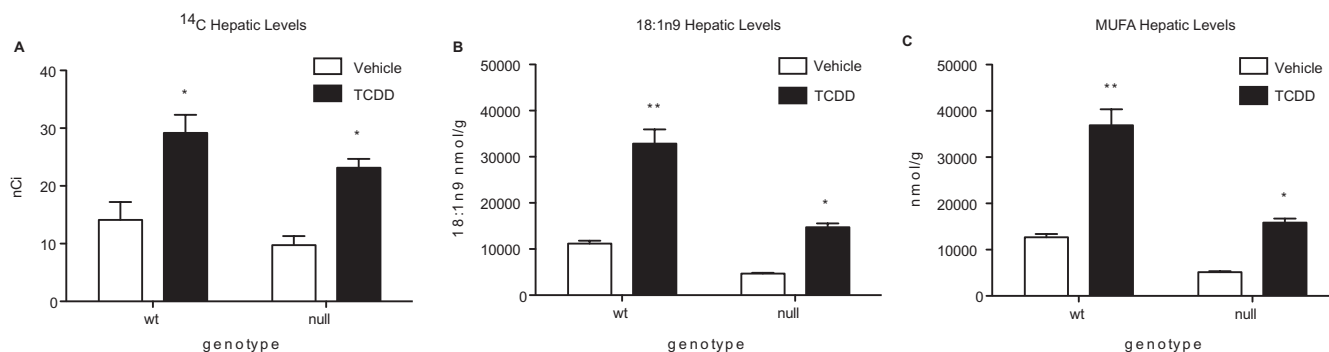


FIG. 2. Hepatic ^{14}C and lipid levels in *Scd1* wild type and null mice 120 h postdose with 30 $\mu\text{g}/\text{kg}$ TCDD. (A) ^{14}C -levels were measured in lipid extracts by liquid scintillation counting after gavage with 2 μCi ^{14}C -oleate 4 h prior to sacrifice. Gas chromatography mass spectrometry analysis of hepatic oleate (18:1n9) (B) and monounsaturated fatty acid (C) levels (expressed in nmol/g) in *Scd1* wild type and null mice 168 h after oral gavage with 30 $\mu\text{g}/\text{kg}$ TCDD (Angrish *et al.*, 2011). * $p < 0.05$ for TCDD compared with vehicle, ** $p < 0.05$ for *Scd1* wild type TCDD compared with *Scd1* null mice TCDD. Bars represent mean \pm SEM, $n = 5$.

Watkins, 2008) and insulin sensing (Wu *et al.*, 2006), solute carrier family 27 (FA transporter), member 1 (*Slc27a1*) expression (2.3-fold in duodenum, -5.8 -fold in jejunum) occurs primarily in muscle and adipose tissue making its role in other tissues uncertain.

Endothelial lipases hydrolyze serum lipids absorbed by the intestine. The resulting products are taken up by the liver via facilitated transport or receptor-mediated endocytosis. TCDD induced hepatic long-chain FA uptake of family members *Cd36* (4.4-fold), solute carrier family 27 (FA transporter), member 3 (*Slc27a3*, 2.7-fold), *Slc27a4* (3.0-fold), and *Ldlr* (3.2-fold) (Table 3). Hydrolytic cleavage of TAG by cytosolic lipases further adds FAs to the hepatic pool. TCDD induced lipoprotein lipase (*Lpl*, 3.2-fold), pancreatic colipase (*Clps*, 2.6-fold), pancreatic lipase-related protein 1 (*Pnliprp1*, 3.7-fold), and monoglyceride lipase (*Mgl1*, 1.4-fold), but repressed patatin-like phospholipase domain containing 3 (*Pnpla3*, 3.3-fold) (Table 3). Interestingly, sequence variations in *PNPLA3* are associated with hepatic TAG content and nonalcoholic fatty liver disease (NAFLD) in humans (Romeo *et al.*, 2008).

Intracellular FAs are directed to TAG biosynthetic and β -oxidation pathways by Fabps. *Fabp1* and *4* were induced 2.9- and 1.4-fold, respectively. However, TCDD repressed hepatic mitochondrial medium- and long-chain acyl-CoA synthetase genes (*Acsml-4* and *Acsll1*, 3-4, repressed 1.3 to 2.3-fold) that activate FAs for transport into the inner membrane space for subsequent β -oxidation (Table 3). These gene expression changes are consistent with the reported inhibition of mitochondrial β -oxidation by TCDD (Lakshman *et al.*, 1991; Lee *et al.*, 2010). Furthermore, TCDD induced the expression of hepatic TAG biosynthesis genes (monoacylglycerol O-acyltransferase 1 and 2 [*Mogat1* and *Mogat2*] and diacylglycerol O-acyltransferase 1 and 2 [*Dgat1* and *Dgat2*] induced 3.6-, 3.0-, 1.6-, and 1.3-fold, respectively), consistent with hepatic TAG accumulation (Angrish *et al.*, 2011; Kopec *et al.*, 2010).

Hepatic differential gene expression is also consistent with TCDD-elicited disruption of carbohydrate catabolism (Table 3). TCDD induced hexokinase 3 (*Hk3*) 2.2-fold, which catalyzes the irreversible phosphorylation of glucose to glucose-6-phosphate (G6P). In contrast, genes involved in gluconeogenesis (pyruvate carboxylase [*Pcx*] -1.3 -fold, phosphoenolpyruvate carboxykinase 1, cytosolic [*Pck1*] -2.0 -fold, and glucose-6-phosphatase, catalytic [*G6pc*] -2.7 -fold) and glycogen synthesis (glucokinase [*Gck*] -1.5 -fold and glycogen synthase 2 [*Gys2*] -1.5 -fold) were repressed. Similarly, genes that provide FA synthesis substrates, such as ATP-citrate lyase (*Acly* -2.6 -fold) and acetyl-CoA carboxylase (*Acaca* -1.4 -fold), and fatty acid synthetase (*Fasn*, -2.8 -fold) were repressed (Table 3). These changes are consistent with the lack of a dose-dependent increase in hepatic TFAs through *de novo* lipogenesis in mice fed with carbohydrate-adjusted diets. Furthermore, reported changes in hepatic gene expression are consistent with hepatic TCDD reported in the same model (Boverhof *et al.*, 2006).

DISCUSSION

Hepatic steatosis can result from the disruption of multiple processes involved in lipid and carbohydrate uptake, metabolism, and efflux. Our studies provided evidence that dietary fat, rather than carbohydrate, is an important lipid source in TCDD-elicited steatosis in mice. Computational DRE search, ChIP-chip, and gene expression (Dere *et al.*, 2011b) data indicate AhR activation results in a coordinated response involving the digestive, circulatory, and hepatic systems (Fig. 3). This suggests any ligand (e.g., chemical, drug, endogenous substance, and natural product) capable of activating the AhR may enhance dietary fat processing and transport, although continuous exposure may be required.

Increases in hepatic ^{14}C levels clearly demonstrated diet as a source of lipids in TCDD-elicited hepatic steatosis. Previous studies have implicated the mobilization of peripheral adipose

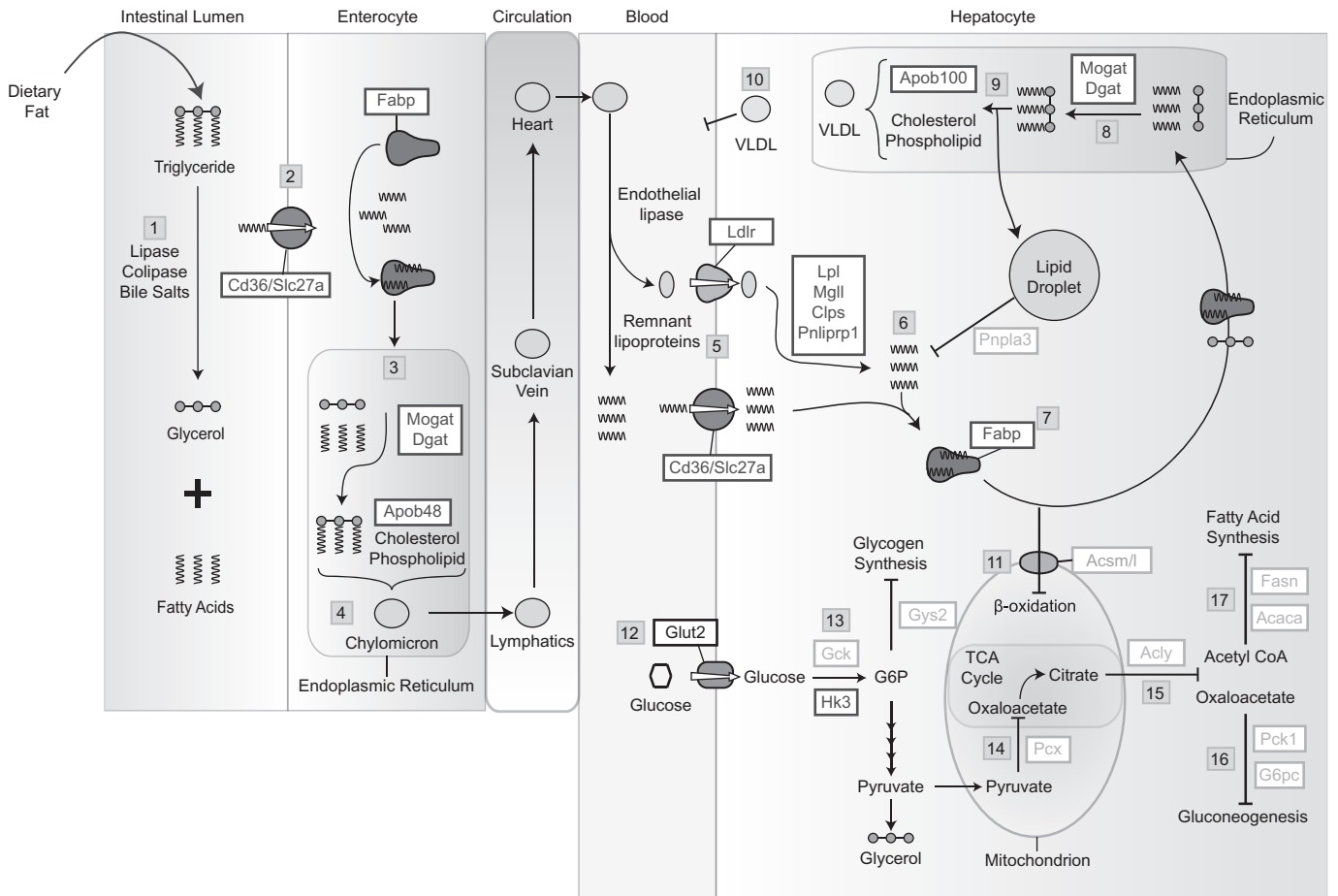


FIG. 3. AhR-mediated increase in dietary lipid in TCDD-elicited hepatic steatosis. Steps 1–4: Fat absorption by the intestinal epithelium and export to the circulatory system. Steps 5–11: Enhanced hepatic fatty acid uptake and storage. Inhibition of efflux and β -oxidation-mediated degradation pathways. Steps 12–17: Hepatic glucose metabolism including glycogen synthesis, gluconeogenesis and fatty acid synthesis are inhibited. Lines with arrowheads indicate reaction/pathway direction. Lines with blunted ends indicate reactions/pathways that are inhibited. Red boxes indicate induced gene expression. Green boxes indicate repressed gene expression. A more detailed description is provided in the Discussion section.

tissue based on increased serum 16:0, 18:1, 18:2, and 18:3 FFA levels and their abundance in adipose tissue (Albro *et al.*, 1978; Lakshman *et al.*, 1991; Pohjanvirta *et al.*, 1990). However, these FFAs also represent the primary lipids in chow (Supplementary table 3). Furthermore, increases in oleate, the primary MUFA in rodent chow, and hepatic ^{14}C levels in *Scd1* null mice provide further evidence of a role for dietary fat in AhR-mediated steatosis.

Complementary gene expression analysis is consistent with a role for the AhR in mediating hepatic accumulation of dietary lipids (Fig. 3). FFAs hydrolyzed by pancreatic and gastric lipases, colipases, and bile salts passively diffuse ($\text{FA} < 16\text{C}$) and are actively transported ($\text{FA} > 16\text{C}$) into enterocytes by *Cd36* and *Slc27a4* that were induced by TCDD (steps 1–3). A role for *Cd36* in intestinal lipid clearance and FFA uptake has been demonstrated in null mice (Drover *et al.*, 2005), whereas *Slc27a4* (*Fatp4*) is associated with obesity in humans (Gertow *et al.*, 2004). Once intracellular, FA binding proteins (*Fabps*) sequester FFAs to prevent their transport back into the intestinal lumen

and target them to specific organelles (Smathers and Petersen, 2011). TCDD inducible *Fabp1*, unlike other family members, binds two rather than one FA, as well as other small hydrophobic ligands (Storch and Thumser, 2010), and is involved in intestinal FA processing and chylomicron maturation (step 4) (Neeli *et al.*, 2007; Storch and McDermott, 2009). Although intestinal lipid absorption is highly efficient (Labonte *et al.*, 2008; Simon *et al.*, 2011), AhR activation may enhance intestinal lipid processing and efflux, consistent with TCDD-induced increases in serum FFAs and TAGs (Boverhof *et al.*, 2006).

The concurrent induction of several hepatic genes associated with lipid transport, processing, and metabolism further promotes steatosis (Fig. 3). *Ldlr*, *Cd36*, and *Slc27a* actively transport increased circulating FFAs, chylomicrons, and lipoprotein remnants into the liver (step 5). TCDD also induced *Lpl*, monoglyceride lipase *Mgll*, *Pnliprp1*, and pancreatic colipase (*Clps*) that hydrolyze intracellular lipoprotein remnants to further increase the intracellular FA pool (step 6). Induced *Fabp1* binds

and sequesters intracellular FAs and targets them for TAG synthesis (Atshaves *et al.*, 2010). *Mogat1/2* and *Dgat1/2*, induced by TCDD, then facilitate hepatic TAG biosynthesis (steps 7 and 8). TAGs are stored in lipid droplets (step 9), or incorporated into VLDLs (step 10). However, TCDD inhibits VLDL secretion (step 10) (Lee *et al.*, 2010), consistent with AhR-mediated increases in hepatic TAG and vacuolization (Angrish *et al.*, 2011; Miyazaki *et al.*, 2000).

Fabp1 also targets FAs for mitochondrial β -oxidation (Atshaves *et al.*, 2010). TCDD inhibits FA oxidation (Lakshman *et al.*, 1991; Lee *et al.*, 2010) possibly by inhibiting transport into mitochondria, further adding to hepatic FA accumulation. More specifically, TCDD inhibits medium- and long-chain FA mitochondrial acyl-CoA synthetase gene expression (*Acsml-4*, *Ascl1*, and *3-4*) (step 11) that is required for transport across the mitochondrial matrix via carnitine for subsequent β -oxidation. Yet, TCDD induced ketone body accumulation *in vitro* (Lakshman *et al.*, 1991), suggesting an intact carnitine pathway. Nonetheless, plasma ketones do not increase in response to TCDD exposure *in vivo* (Pohjanvirta and Tuomisto, 1994) and requires additional investigation.

The inability of carbohydrate diets to enhance hepatic steatosis appears to involve TCDD dysregulation of carbohydrate metabolism gene expression (step 12). For example, anabolic pathways typically dominate in fed animals, yet TCDD decreased glucokinase (*Gck*) and glycogen synthase (*Gys2*), suggesting suppression of hepatic glycogen synthesis (step 13). Glucokinase is the predominant enzyme regulating hepatic glucose metabolism in response to nutritional states such as refeeding and insulin stimulation (Agius, 2008). Although TCDD induced hexokinase (*Hk3*), this enzyme is expressed at low levels in hepatocytes, yet exhibits compensatory induction following glucokinase repression, as found in liver cirrhosis (Lowe *et al.*, 1998). TCDD also inhibited mitochondrial pyruvate carboxylase (*Pcx*) that converts pyruvate into oxaloacetate, suggesting flux toward glycerol production to support hepatic TAG production leading to greater sequestration of hepatic FA. Metabolomic studies also report TCDD increases hepatic glycerol levels (Forgacs *et al.*, 2012) and that TCDD treatment prevents glycerol ketogenesis without affecting esterification to TAG (Lakshman *et al.*, 1991).

TCDD suppressed phosphoenolpyruvate carboxykinase (*Pck1*) and glucose-6 phosphatase (*G6pc*) expression, key regulators of gluconeogenesis (steps 14 and 16). These genes are commonly regulated by peroxisome proliferator-activated receptor γ (PPAR γ) coactivator 1 α (PGC-1 α) (Burgess *et al.*, 2006) that is functionally impaired by AhR-mediated induction of TCDD-inducible poly(ADP-ribose) polymerase 7, PARP7 (TiPARP) (Diani-Moore *et al.*, 2010). TCDD also repressed ATP-citrate lyase (*Acly*), which converts citrate to oxaloacetate and acetyl-CoA (step 15). Acetyl CoA is critical for *de novo* FA synthesis by *Fasn* (step 17), which was dose dependently repressed by TCDD, TCDF, and PCB126 (Kopeck *et al.*, 2011).

These gene expression changes are consistent with TCDD-mediated inhibition of gluconeogenesis (Viluksela *et al.*, 1999),

de novo lipogenesis (Lakshman *et al.*, 1988), and FA oxidation, but roughly concordant with DRE distributions and AhR ChIP-chip peaks (Table 3). This may be partially explained by AhR interactions with other signaling pathways involved in hepatic glucose and FA metabolism regulation including PPARs (Table 3), *Pgc1 α* (Diani-Moore *et al.*, 2010), Forkhead box O1 (Foxo1) (Matsumoto *et al.*, 2007), and hepatocyte nuclear factor 4, α (HNF4 α) (Hardwick *et al.*, 2009). Evidence suggests AhR and PPAR signaling pathways interact (Alexander *et al.*, 1998; Liu and Matsumura, 1995; Remillard and Bunce, 2002) to alter PPAR expression (Wang *et al.*, 2011). Other studies identified overrepresentation of PPAR and HNF4 α binding motifs in ChIP-chip regions of AhR enrichment that lack DRE cores, suggesting AhR binding to DNA independent of DREs (Dere *et al.*, 2011b; Murray *et al.*, 2010). For example, AhR interacts with chicken ovalbumin upstream promoter transcription factor (COUP-TF) (Klinge *et al.*, 2000), and COUP-TF is reported to antagonize HNF4 α -mediated responses by binding to HNF4 α response elements (Mietus-Snyder *et al.*, 1992). Consequently, AhR-COUP-TF complexes binding to HNF4 α response elements may inhibit HNF4 α -regulated lipid transport, metabolism, and gene expression and contribute to TCDD-elicited steatosis (Dere *et al.*, 2011b). Interestingly, hepatic steatosis has been reported in HNF4 α null mice (Hayhurst *et al.*, 2001).

Collectively, our data indicate that TCDD-mediated hepatic steatosis involves enhanced uptake of dietary fat suggesting a novel endogenous role for the AhR. Other ligands including endogenous metabolites (indoles, tetrapyrroles, and arachidonic acid metabolites), and natural products (e.g., vegetable-, fruit-, and tea-derived indole and flavonoid metabolites) (Denison and Nagy, 2003; Nguyen and Bradfield, 2008) also activate the AhR providing a possible selective evolutionary advantage that optimizes fat absorption to maximize energy intake. Interactions with other nuclear receptors and transcription factors can further impact energy homeostasis and lipid metabolism, transport, and deposition. However, persistent AhR activation in combination with the consumption of a high-fat diet may also have adverse health implications for fatty liver and its associated diseases including NAFLD, metabolic syndrome, and diabetes. Preliminary studies indicate AhR activation increases TFA levels in human primary hepatocytes (data not shown), although further studies are needed to elucidate species-specific differences in AhR-mediated effects including steatosis.

SUPPLEMENTARY DATA

Supplementary data are available online at <http://toxsci.oxfordjournals.org/>.

FUNDING

National Institute of Environmental Health Sciences Superfund Research Program (P42ES04911).

ACKNOWLEDGMENTS

We thank Claudia Dominici for technical support and Dr Anna Kopec, Rance Nault, and Agnes Forgacs for critical review.

REFERENCES

- Albro, P. W., Corbett, J. T., Harris, M., and Lawson, L. D. (1978). Effects of 2,3,7,8-tetrachlorodibenzo-p-dioxin on lipid profiles in tissue of the Fischer rat. *Chem. Biol. Interact.* **23**, 315–330.
- Alexander, D. L., Ganem, L. G., Fernandez-Salguero, P., Gonzalez, F., and Jefcoate, C. R. (1998). Aryl-hydrocarbon receptor is an inhibitory regulator of lipid synthesis and of commitment to adipogenesis. *J. Cell Sci.* **111**(Pt 22), 3311–3322.
- Angrish, M. M., Jones, A. D., Harkema, J. R., and Zacharewski, T. R. (2011). Aryl hydrocarbon receptor-mediated induction of stearoyl-CoA desaturase 1 alters hepatic fatty acid composition in TCDD-elicited steatosis. *Toxicol. Sci.* **124**, 299–310.
- Atshaves, B. P., Martin, G. G., Hostetler, H. A., McIntosh, A. L., Kier, A. B., and Schroeder, F. (2010). Liver fatty acid-binding protein and obesity. *J. Nutr. Biochem.* **21**, 1015–1032.
- Boron, W., and Boulpaep, E. (2008). *Medical Physiology*. Saunders, Philadelphia, PA.
- Boverhof, D. R., Burgoon, L. D., Tashiro, C., Sharratt, B., Chittim, B., Harkema, J. R., Mendrick, D. L., and Zacharewski, T. R. (2006). Comparative toxicogenomic analysis of the hepatotoxic effects of TCDD in Sprague Dawley rats and C57BL/6 mice. *Toxicol. Sci.* **94**, 398–416.
- Burgess, S. C., Leone, T. C., Wende, A. R., Croce, M. A., Chen, Z., Sherry, A. D., Malloy, C. R., and Finck, B. N. (2006). Diminished hepatic gluconeogenesis via defects in tricarboxylic acid cycle flux in peroxisome proliferator-activated receptor gamma coactivator-1alpha (PGC-1alpha)-deficient mice. *J. Biol. Chem.* **281**, 19000–19008.
- Denison, M. S., and Nagy, S. R. (2003). Activation of the aryl hydrocarbon receptor by structurally diverse exogenous and endogenous chemicals. *Annu. Rev. Pharmacol. Toxicol.* **43**, 309–334.
- Denison, M. S., Soshilov, A. A., He, G., DeGroot, D. E., and Zhao, B. (2011). Exactly the same but different: Promiscuity and diversity in the molecular mechanisms of action of the aryl hydrocarbon (dioxin) receptor. *Toxicol. Sci.* **124**, 1–22.
- Dere, E., Forgacs, A. L., Zacharewski, T. R., and Burgoon, L. D. (2011a). Genome-wide computational analysis of dioxin response element location and distribution in the human, mouse, and rat genomes. *Chem. Res. Toxicol.* **24**, 494–504.
- Dere, E., Lo, R., Celius, T., Matthews, J., and Zacharewski, T. R. (2011b). Integration of genome-wide computation DRE Search, AhR ChIP-chip and gene expression analyses of TCDD-elicited responses in the mouse liver. *BMC Genomics* **12**, 365.
- Diani-Moore, S., Ram, P., Li, X., Mondal, P., Youn, D. Y., Sauve, A. A., and Rifkind, A. B. (2010). Identification of the aryl hydrocarbon receptor target gene TipARP as a mediator of suppression of hepatic gluconeogenesis by 2,3,7,8-tetrachlorodibenzo-p-dioxin and of nicotinamide as a corrective agent for this effect. *J. Biol. Chem.* **285**, 38801–38810.
- Drover, V. A., Ajmal, M., Nassir, F., Davidson, N. O., Nauli, A. M., Sahoo, D., Tso, P., and Abumrad, N. A. (2005). CD36 deficiency impairs intestinal lipid secretion and clearance of chylomicrons from the blood. *J. Clin. Invest.* **115**, 1290–1297.
- Forgacs, A. L., Kent, M. N., Makley, M. K., Mets, B., DelRaso, N., Jahns, G. L., Burgoon, L. D., Zacharewski, T. R., and Reo, N. V. (2012). Comparative metabolomic and genomic analyses of TCDD-elicited metabolic disruption in mouse and rat liver. *Toxicol. Sci.* **125**, 41–55.
- Gertow, K., Pietilainen, K. H., Yki-Jarvinen, H., Kaprio, J., Rissanen, A., Eriksson, P., Hamsten, A., and Fisher, R. M. (2004). Expression of fatty-acid-handling proteins in human adipose tissue in relation to obesity and insulin resistance. *Diabetologia* **47**, 1118–1125.
- Hankinson, O. (1995). The aryl hydrocarbon receptor complex. *Annu. Rev. Pharmacol. Toxicol.* **35**, 307–340.
- Hardwick, J. P., Osei-Hyiaman, D., Wiland, H., Abdelmegeed, M. A., and Song, B. J. (2009). PPAR/RXR regulation of fatty acid metabolism and fatty acid omega-hydroxylase (CYP4) isozymes: Implications for prevention of lipotoxicity in fatty liver disease. *PPAR Res.* **2009**, 952734.
- Hayhurst, G. P., Lee, Y. H., Lambert, G., Ward, J. M., and Gonzalez, F. J. (2001). Hepatocyte nuclear factor 4alpha (nuclear receptor 2A1) is essential for maintenance of hepatic gene expression and lipid homeostasis. *Mol. Cell Biol.* **21**, 1393–1403.
- Iqbal, J., and Hussain, M. M. (2009). Intestinal lipid absorption. *Am. J. Physiol. Endocrinol. Metab.* **296**, E1183–E1194.
- Klinge, C. M., Kaur, K., and Swanson, H. I. (2000). The aryl hydrocarbon receptor interacts with estrogen receptor alpha and orphan receptors COUP-TFI and ERRalpha1. *Arch. Biochem. Biophys.* **373**, 163–174.
- Kopec, A. K., Burgoon, L. D., Ibrahim-Aibo, D., Mets, B. D., Tashiro, C., Potter, D., Sharratt, B., Harkema, J. R., and Zacharewski, T. R. (2010). PCB153-elicited hepatic responses in the immature, ovariectomized C57BL/6 mice: Comparative toxicogenomic effects of dioxin and non-dioxin-like ligands. *Toxicol. Appl. Pharmacol.* **243**, 359–371.
- Kopec, A. K., D'Souza, M. L., Mets, B. D., Burgoon, L. D., Reese, S. E., Archer, K. J., Potter, D., Tashiro, C., Sharratt, B., Harkema, J. R., et al. (2011). Non-additive hepatic gene expression elicited by 2,3,7,8-tetrachlorodibenzo-p-dioxin (TCDD) and 2,2',4,4',5,5'-hexachlorobiphenyl (PCB153) co-treatment in C57BL/6 mice. *Toxicol. Appl. Pharmacol.* **256**, 154–167.
- Labonte, E. D., Camarota, L. M., Rojas, J. C., Jandacek, R. J., Gilham, D. E., Davies, J. P., Ioannou, Y. A., Tso, P., Hui, D. Y., and Howles, P. N. (2008). Reduced absorption of saturated fatty acids and resistance to diet-induced obesity and diabetes by ezetimibe-treated and Npc111-/- mice. *Am. J. Physiol. Gastrointest. Liver Physiol.* **295**, G776–G783.
- Lakshman, M. R., Campbell, B. S., Chirtel, S. J., and Ekarohita, N. (1988). Effects of 2,3,7,8-tetrachlorodibenzo-p-dioxin (TCDD) on de novo fatty acid and cholesterol synthesis in the rat. *Lipids* **23**, 904–906.
- Lakshman, M. R., Ghosh, P., and Chirtel, S. J. (1991). Mechanism of action of 2,3,7,8-tetrachlorodibenzo-p-dioxin on intermediary metabolism in the rat. *J. Pharmacol. Exp. Ther.* **258**, 317–319.
- Lee, C. C., Yao, Y. J., Chen, H. L., Guo, Y. L., and Su, H. J. (2006). Fatty liver and hepatic function for residents with markedly high serum PCDD/Fs levels in Taiwan. *J. Toxicol. Environ. Health A* **69**, 367–380.
- Lee, J. H., Wada, T., Febbraio, M., He, J., Matsubara, T., Lee, M. J., Gonzalez, F. J., and Xie, W. (2010). A novel role for the dioxin receptor in fatty acid metabolism and hepatic steatosis. *Gastroenterology* **139**, 653–663.
- Liu, P. C., and Matsumura, F. (1995). Differential effects of 2,3,7,8-tetrachlorodibenzo-p-dioxin on the “adipose-type” and “brain-type” glucose transporters in mice. *Mol. Pharmacol.* **47**, 65–73.
- Lowes, W., Walker, M., Alberti, K. G., and Agius, L. (1998). Hexokinase isoenzymes in normal and cirrhotic human liver: Suppression of glucokinase in cirrhosis. *Biochim. Biophys. Acta* **1379**, 134–142.
- Matsumoto, M., Poci, A., Rossetti, L., Depinho, R. A., and Accili, D. (2007). Impaired regulation of hepatic glucose production in mice lacking the forkhead transcription factor Foxo1 in liver. *Cell Metab.* **6**, 208–216.
- Mietus-Snyder, M., Sladek, F. M., Ginsburg, G. S., Kuo, C. F., Ladas, J. A., Darnell, J. E., Jr. and Karathanasis, S. K. (1992). Antagonism between apolipoprotein AI regulatory protein 1, Ear3/COUP-TF, and hepatocyte nuclear factor 4 modulates apolipoprotein CIII gene expression in liver and intestinal cells. *Mol. Cell Biol.* **12**, 1708–1718.
- Miyazaki, M., Kim, Y. C., Gray-Keller, M. P., Attie, A. D., and Ntambi, J. M. (2000). The biosynthesis of hepatic cholesterol esters and triglycerides is impaired in mice with a disruption of the gene for stearoyl-CoA desaturase 1. *J. Biol. Chem.* **275**, 30132–30138.

- Miyazaki, M., Man, W. C., and Ntambi, J. M. (2001). Targeted disruption of stearoyl-CoA desaturase1 gene in mice causes atrophy of sebaceous and meibomian glands and depletion of wax esters in the eyelid. *J. Nutr.* **131**, 2260–2268.
- Murray, I. A., Morales, J. L., Flaveny, C. A., Dinatale, B. C., Chiaro, C., Gowdahalli, K., Amin, S., and Perdew, G. H. (2010). Evidence for ligand-mediated selective modulation of aryl hydrocarbon receptor activity. *Mol. Pharmacol.* **77**, 247–254.
- Neeli, I., Siddiqi, S. A., Siddiqi, S., Mahan, J., Lagakos, W. S., Binas, B., Gheyi, T., Storch, J., and Mansbach, C. M., II. (2007). Liver fatty acid-binding protein initiates budding of pre-chylomicron transport vesicles from intestinal endoplasmic reticulum. *J. Biol. Chem.* **282**, 17974–17984.
- Nguyen, L. P., and Bradfield, C. A. (2008). The search for endogenous activators of the aryl hydrocarbon receptor. *Chem. Res. Toxicol.* **21**, 102–116.
- Pohjanvirta, R., Sankari, S., Kulju, T., Naukkarinen, A., Ylinen, M., and Tuomisto, J. (1990). Studies on the role of lipid peroxidation in the acute toxicity of TCDD in rats. *Pharmacol. Toxicol.* **66**, 399–408.
- Pohjanvirta, R., and Tuomisto, J. (1994). Short-term toxicity of 2,3,7,8-tetrachlorodibenzo-p-dioxin in laboratory animals: Effects, mechanisms, and animal models. *Pharmacol. Rev.* **46**, 483–549.
- Pollenz, R. S., Sattler, C. A., and Poland, A. (1994). The aryl hydrocarbon receptor and aryl hydrocarbon receptor nuclear translocator protein show distinct subcellular localizations in Hepa 1c1c7 cells by immunofluorescence microscopy. *Mol. Pharmacol.* **45**, 428–438.
- Remillard, R. B., and Bunce, N. J. (2002). Linking dioxins to diabetes: Epidemiology and biologic plausibility. *Environ. Health Perspect.* **110**, 853–858.
- Romeo, S., Kozlitina, J., Xing, C., Pertsemlidis, A., Cox, D., Pennacchio, L. A., Boerwinkle, E., Cohen, J. C., and Hobbs, H. H. (2008). Genetic variation in PNPLA3 confers susceptibility to nonalcoholic fatty liver disease. *Nat. Genet.* **40**, 1461–1465.
- Simon, T., Cook, V. R., Rao, A., and Weinberg, R. B. (2011). Impact of murine intestinal apolipoprotein A-IV expression on regional lipid absorption, gene expression, and growth. *J. Lipid Res.* **52**, 1984–1994.
- Smathers, R. L., and Petersen, D. R. (2011). The human fatty acid-binding protein family: Evolutionary divergences and functions. *Hum. Genomics* **5**, 170–191.
- Storch, J., and McDermott, L. (2009). Structural and functional analysis of fatty acid-binding proteins. *J. Lipid Res.* **50**, S126–S131.
- Storch, J., and Thumser, A. E. (2010). Tissue-specific functions in the fatty acid-binding protein family. *J. Biol. Chem.* **285**, 32679–32683.
- Swedenborg, E., Ruegg, J., Makela, S., and Pongratz, I. (2009). Endocrine disruptive chemicals: Mechanisms of action and involvement in metabolic disorders. *J. Mol. Endocrinol.* **43**, 1–10.
- Vandesompele, J., De Preter, K., Pattyn, F., Poppe, B., Van Roy, N., De Paepe, A., and Speleman, F. (2002). Accurate normalization of real-time quantitative RT-PCR data by geometric averaging of multiple internal control genes. *Genome Biol.* **3**, 34.
- Viluksela, M., Unkila, M., Pohjanvirta, R., Tuomisto, J. T., Stahl, B. U., Rozman, K. K., and Tuomisto, J. (1999). Effects of 2,3,7,8-tetrachlorodibenzo-p-dioxin (TCDD) on liver phosphoenolpyruvate carboxykinase (PEPCK) activity, glucose homeostasis and plasma amino acid concentrations in the most TCDD-susceptible and the most TCDD-resistant rat strains. *Arch. Toxicol.* **73**, 323–336.
- Wang, C., Xu, C. X., Krager, S. L., Bottum, K. M., Liao, D. F., and Tischkau, S. A. (2011). Aryl hydrocarbon receptor deficiency enhances insulin sensitivity and reduces PPAR-alpha pathway activity in mice. *Environ. Health Perspect.* **119**, 1739–1744.
- Watkins, P. A. (2008). Very-long-chain acyl-CoA synthetases. *J. Biol. Chem.* **283**, 1773–1777.
- Wu, Q., Ortegon, A. M., Tsang, B., Doege, H., Feingold, K. R., and Stahl, A. (2006). FATP1 is an insulin-sensitive fatty acid transporter involved in diet-induced obesity. *Mol. Cell Biol.* **26**, 3455–3467.